AD-A065 093 WASHINGTON UNIV SEATTLE DEPT OF MECHANICAL ENGINEERING F/G 20/11
A CRITICAL EXAMINATION OF A NUMERICAL FRACTURE DYNAMIC CODE.(U)
FEB 79 L HODULAK, A S KOBAYSHI, A F EMERY N00014-76-C-0060
UNCLASSIFIED TR-34 NL

1 OF 1
ADA
065093

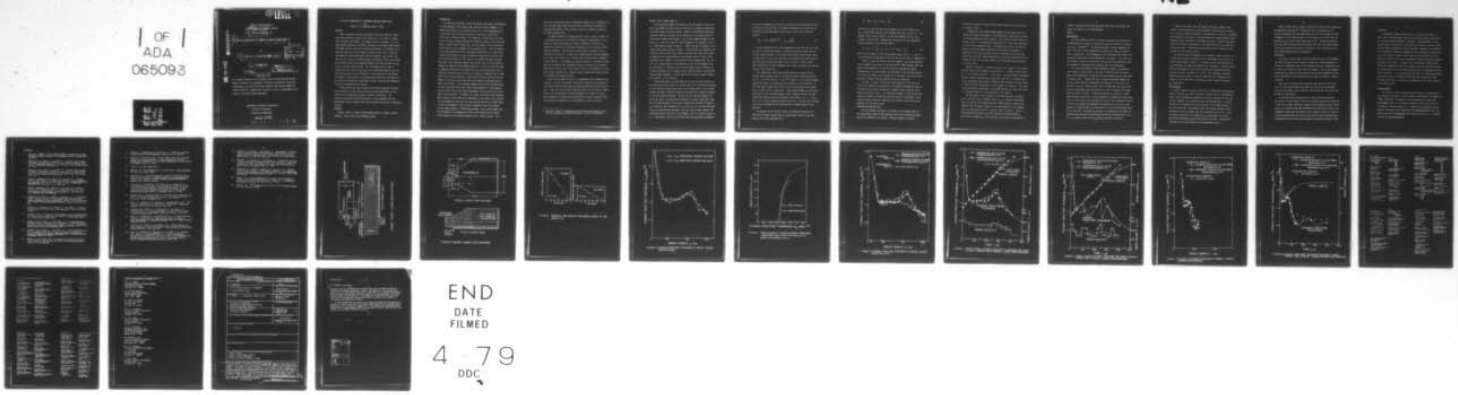

END
DATE
FILMED
4 79
DDC

(12) B.S. LEVEL II

Office of Naval Research

(15) Contract N00014-76-C-0060, NR 064-478

(9) Technical Report No. 34

(6) # A CRITICAL EXAMINATION OF A NUMERICAL FRACTURE DYNAMIC CODE

by

(10) L. Hodulak, A.S. Kobayashi, A.F. Emery

(11) February 1979

(12) 30 pp.

(14) TR-34

The research reported in this technical report was made possible through support extended to the Department of Mechanical Engineering, University of Washington, by the Office of Naval Research under Contract N00014-76-C-0060, NR 064-478. Reproduction in whole or in part is permitted for any purpose of the United States Government.

Department of Mechanical Engineering

College of Engineering

University of Washington

A CRITICAL EXAMINATION OF A NUMERICAL FRACTURE DYNAMIC CODE

by

L. Hodulak, A.S. Kobayashi and A.F. Emery

ABSTRACT

After upgrading the energy dissipation algorithm, numerical experiments were conducted to assess the reliability of the explicit dynamic finite element code, HCRACK. Two dynamic fracture specimens, i.e., the wedge-loaded rectangular DCB (RDCB) specimen and the wedge-loaded tapered DCB (TDCB) specimen, which were studied experimentally by Kalthoff et al, were then analyzed with this updated fracture dynamic code. Using the experimentally determined dynamic fracture toughness, K_{ID}, versus crack velocity, $\dot{a}$, relation, the RDCB specimen was analyzed first by the "propagation method" where good agreements between calculated and measured K_{ID} versus a relations were observed. The calculated a versus time, t, relation was then used as input data in the "generation method" where the resultant K_{ID} were virtually identical to those obtained in the propagation method. Error analyses of the generation method were also made first by using the experimentally determined a versus t relation and secondly by artificially perturbing this relation.

A TDCB specimen was then analyzed with both the propagation and generation methods by using the K_{ID} versus $\dot{a}$ relation established for this specimen and the measured a versus t relation, respectively. The computed K_{ID} obtained by both methods were in good agreement with the experimental results, showing that either approach can be used in analyzing fracture.

KEYWORDS

Dynamic fracture, dynamic finite element analysis, dynamic fracture toughness, crack arrest stress intensity factor.

INTRODUCTION

For the past three years, two of the authors have used a two-dimensional elasto-dynamic finite element code, which was based on HONDO [1], to compute the dynamic stress intensity factor for a crack propagating with a prescribed velocity [2-5] by applying to each node a nodal force sufficient to release the node. This numerical procedure was later modified to include a startup procedure for computing dynamic stress intensity factor, dynamic energy release rate, fracture energy, kinetic energy and strain energy at each increment of crack advance [6,7]. Also the impulse stress waves generated by the instantaneous application of a nodal force to model the release of a crack-tip node was reduced by varying the force over the time necessary for the crack tip to advance one nodal distance. Physically, this procedure models a more gradual transit of the crack-tip between two adjacent finite element nodes and is similar to that developed by Keegstra [8-10] with the exception that our restraining nodal force is completely eliminated when the crack-tip reaches its adjacent node. Other nodal force release mechanisms include those of Malluck and King [11] and Rydholm, Fredriksson and Nilsson [12] with different postulated rates of nodal force release. The dissipated energy during a crack extension based on any of the above three nodal force release mechanism is then computed from the nodal force versus nodal displacement relation during this incremental crack extension. In general this nodal force versus nodal displacement relation is non-linear and is goverened by the dynamic state surrounding the propagating crack tip thus requiring the monitoring of nodal force or nodal displacement or both at every incremental time in the dynamic finite element analysis. Interestingly enough, recent studies showed that the differences in the mechanism of nodal force release [13,14] caused little changes in the resultant dynamic stress intensity factor. It is

thus of no surprise that good to excellent agreements were claimed by all [6,11,12] when these three crack tip energy dissipation procedures for computing the dynamic stress intensity factor was checked by analyzing the Broberg problem [15].

The above procedure of computing dynamic stress intensity factor for a crack whose velocity is prescribed to be equal to measured one in a dynamically fracturing specimen was termed "generation calculation" by Kanninen [16,17] who also expressed reservations on the accuracy of this numerical approach. The "propagation calculation" in contrast to the "generation calculation" is based on an assumed dynamic fracture toughness, K_{ID}, versus crack velocity, $\dot{a}$, relation which is then used to propagate a crack [16-23].* The assumed K_{ID} versus $\dot{a}$ relation is considered correct when the calculated crack propagation history coincides with the experimental data, and the K_{ID} at crack arrest, if any, is considered to be the crack arrest toughness, K_{Ia}, sought by some in predicting fracture arrest of a dynamically propagating crack.

While one can debate the merits of propagation versus generation calculations, only one study which involved both propagation and generation calculation using the same numerical algorithm [23] has been published to-date. Since the limited study in Reference [23] did not provide a comprehensive error assessment of the two procedures, this paper will report on our comparative studies using two Araldite B fracture specimens which were analyzed by Kalthoff et al by the method of caustics [24,25].

---

* Note that Keegstra in References [8,9,10] used the propagation calculation to compute K_{ID} versus a relations in fracturing specimens.

DYNAMIC FINITE ELEMENT ANALYSIS

In the previous studies cited above [6,26], the dynamic fracture dynamic code HCRACK was shown to be an efficient and inexpensive method for simulating dynamic fracture problems. Numerical experiments proved that reasonable numerical accuracy can be obtained by using coarse meshes of conventional elements (see Figures 1 and 2) and a moderate number of time steps, e.g., about 150 steps for crack propagation and subsequent arrest in a RDCB specimen shown in Figure 1. Unlike the implicit dynamic finite element codes used by others, however, it was difficult to accurately prescribe the rate of nodal force release since the input nodal force would not generally be in equilibrium with the dynamic state of stress in the adjoining finite elements in this explicit finite element code. As a result, an in-depth study on the performance of our fracture dynamic code was conducted for different crack tip force release rates, different calculation procedures for the dynamic stress intensity factor, and different finite element breakdown. A brief description of some of these findings are presented in the following.

As mentioned above, the algorithm for artificially prescribing an input nodal force at the crack tip for each time step for prescribed decrease in the resultant residual nodal force in the dynamic code is not straightforward and often a complete release of the nodal force cannot be achieved in the prescribed time period. The basis of the numerical method is to define the force, F_n^i which must be applied to a node at time step n such that the time variation of the stress follows the form shown on figure 3. In an implicit code, application of F_n would result in the same calculated force at the end of the time step. With the explicit code, however, the calculated force at the end of the increment, F_n^0, will rarely be equal to F_n^i. Accordingly, the force at the next time step F_{n+1}^i must be adjusted

not only to compensate for the error, but also to yield the desired value at the end of the time step. The simplified method used in [26] was replaced by the following equation and typical results are as shown in figure 3.

$$F_{n+1}^{i} = F_{n}^{0} - F_{n+1}^{\text{prescribed}} - \sum_{j=1}^{n} \frac{F_j^i}{2^{n-j+1}} \qquad (1)$$

At the beginning of the crack propagation history when the first crack tip node is relased (see Figure 3), excellent agreement between the prescribed (linear decrease in this case) and actually achieved nodal forces is noted while for the sixth node which was released later (see Figure 3), some deviations between both nodal forces are noted. Initial static equilibrium prior to crack propagation most likely contribute the excellent results in the former case.

Also noteworthy is the recent study by Malluck and King [13] who compared energy release rates for the two distinctly different functions of $F/F_o = [1-b/\Delta]^{3/2}$ and $F/F_o = [1-b/\Delta]^{1/2}$, where b is the distance between hypothetical crack tip location and the released crack tip node and Δ is the inter-nodal distance and F and F_o are the instantaneous and original crack tip nodal forces, respectively. Their results showed no significant differences in the calculated dynamic stress intensity factors for crack speeds lower than 25 percent of the shear wave velocity, i.e. $c < .25\ c_2$. Our use of a linearly decreasing nodal force, $F/F_o = [1-b/\Delta]$, with constant crack velocity between the two adjoining finite element nodes is thus justified.

The dynamic stress intensity factor was computed directly by the total strain energy released from an instantaneous balance of the total energy of the entire specimen [7] as

$$G_I = 2(E_n - E_{n-1}) / (a_{n+1} - a_n) \quad (2)$$

where E_n, E_{n+1} are the total strain energies for crack lengths of a_n, a_{n+1}, respectively when the crack extended from node n to node n+1. The dynamic stress intensity factor, K_I, was then computed from G_I using Freund's relation [24]. Alternatively the value of G_I was computed by energy dissipated at the released node as

$$G_I = (u_i \Delta F_i + \sum_{i-1}^{m} (u_1 - u_{1-1}) \Delta F_i) / (a_{n+1} - a_n) \quad (3)$$

where m is the number of time steps between nodes n and n+1, u_i and ΔF_i are displacement and decrease of force at the released node n, respectively.

Figure 4, shows the dynamic fracture toughness, K_{ID}, associated with crack propagation and arrest in one of Kalthoff's RDCB specimens [24] computed by both equations (2) and (3) using the "propagation method." Although details of this analysis are described in the following section, the results are shown in this section as an indication that little difference can be noted in the K_{ID} obtained by the two algorithms.

As shown in Figure 4, the forced linear decrease in the crack tip nodal force improved the simulation of the smoothly propagating crack and eliminated the spurious oscillations in dynamic stress intensity factor observed previously [2-5]. It is uncertain, however, to what extent this smoothing procedure may hide the true oscillations of the dynamic stress intensity factor eventually induced by the reflected stress waves which emanated from the running crack.

SPECIMENS AND MATERIAL DATA

The two specimens analyzed by the dynamic finite element code are the wedge-loaded, RDCB and TDCB specimens which were investigated experimentally by Kalthoff et al [24,25]. Specimen geometries of these

Araldite B specimens and their finite element idealizations can be seen in Figures 1 and 2.

Although the rigid loading wedge between the two loading pins will prevent any inward displacement of the loading pins, these pins are free to leave the wedge and travel outwards. The resultant dynamic stress intensity factors in the presence of separating pins could vary significantly during crack propagation [26]. The smaller mass density and the two orders of magnitude larger compliance of the Araldite B specimens in comparison to the steel specimen studied in Reference [26] should have reduced the additional input energy due to any possible separation of the loading pins and thus constant loading pin displacement were prescribed at the pin holes.

Material constants of Araldite B used for this dynamic finite element analysis after [24] are modulus of elasticity $E = 3.38\ GP_a$, Poisson ratio of $\nu = 0.33$ and mass density, $\rho = 1047\ kg/m^3$. The experimentally determined dynamic fracture toughness K_{ID}, versus crack velocity, $\dot{a}$, relations used in the propagation calculations of RDCB and TDCB specimens are both plotted in Figure 5 [24,25] respectively. Crack length as a function of time used in the "generation calculations" of the RDCB specimen was taken from Figure 5 in Reference [24] but is not reproduced in this paper.

For the dynamic crack initiation in the RDCB specimen, the dynamic crack initiation stress intensity factor, K_{IQ}, as reported in Reference [24], was used and the subsequent dynamic stress intensity factors were computed from the energy released at the node adjacent to the reference crack tip node except the set of K_{ID} data noted in Figure 4. Since an experimentally determined K_{IQ} was not reported in Reference [25], a statistically computed K_{IQ}, which was back calculated from the median of

Kalthoff's measured oscillating K_{ID} values [25] after crack arrest, was used in the analysis of the TDCB specimen.

RESULTS

RDCB Specimen

The first numerical analysis involved a propagation calculation for the RDCB specimen of Figure 1 using the K_{ID} versus $\dot{a}$ relation of Figure 5 and a $K_{IQ} = 2.32\ MN\,m^{3/2}$. The resulting dynamic fracture toughness and crack tip motion of this propagation calculation are shown in Figures 6 and 7, respectively. The "propagation" crack tip motion from Figure 7 was then used as input data for the "generation" calculation. This result is not plotted in Figure 6 since the K_{ID} versus $\dot{a}$ relations obtained by both the propagation and generation calculation were indistinguishable.

As an additional numerical experimentation, however, the measured crack length, a, versus time, t, relation of Reference [24] was used as input to the "generation" calculation and the resultant K_{ID} are also shown in Figures 6 and 7. Despite the lack of complete agreement between the two K_{ID} curves obtained by propagation and generation calculation, the shapes of these two curves are very close. Although both K_{ID} curves agree well with experimental data during the first half of dynamic crack propagation as shown in Figure 7, a distinct difference is noted by a second local maximum, which occurs in both propagation and generation calculations prior to crack arrest, but which does not occur in the experimental results. The similarity between the propagation and generation K_{ID} curves is more apparent in Figure 8 where the second maxima in the two calculations occur at the same time. The higher K_{ID} values in the generation calculation at lower measured crack velocities during much of the crack propagation will result in a general shift of two K_{ID} versus $\dot{a}$ relation in Figure 5.

Figure 6 also shows that the computed crack jump distance is 4% shorter of the measured one in the propagation calculation but by definition is equal to measured distance in the generation calculation. Although the propagation calculation is terminated when the computed dynamic stress intensity factor falls below the minimum K_{ID} value in Figure 5, the generation calculation is continued up to the prescribed crack tip length and crack arrest time. Significantly lower dynamic stress intensity at the instant of crack arrest is noted.

The sensitivity of the dynamic stress intensity factor, which is calculated by the generation method, to the instantaneous crack velocity is further demonstrated in Figure 8. In order to assess the sensitivity of K_{ID} obtained by the generation method to the input data, a numerical experiment was conducted by artificially perturbing the smooth experimental curve of the crack tip motion in Figure 8. The result was a severely perturbed K_{ID} also shown in Figure 9, where discrete increases and decreases in crack velocities are followed by local minima and maxima of K_{ID} respectively.

TDCB Specimen

Figure 9 shows the K_{ID} as a function of $\underline{a}$ computed by the propagation method, using the K_{ID} versus $\dot{\underline{a}}$ relation of Figure 5 and by the generation method using experimentally determined $\underline{a}$ versus $\underline{t}$ relations for the TDCB specimen together with experimental data from Reference [25]. A second maximum, which resembles that found previously in the RDCB specimen, in K_{ID} can be observed. The computed crack jump distance obtained by the propagation method is shorter than the experimental one by 12%. In the propagation calculation the computed K_{ID} increased again to a value approaching experimental K_{ID} after the initial crack arrest. Subsequently computed K_{ID} oscillated around the few experimental points.

Figure 10 shows the K_{ID} versus $\underline{t}$ relations obtained by both propagation and generation calculations. Although the two calculated K_{ID} are in excellent agreement with each other except for the initial phase of crack propagation in this TDCB specimen, the calculated K_{ID} are lower than the measured K_{ID} just prior to and after crack arrest. Previous experience with steel TDCB specimens [4,5,26] indicate that this small underestimate could be attributed to the possible separation of the loading pins from the loading wedge during crack propagation.

CONCLUSIONS

The results of the present and of the previous studies using HONDO II show that the dynamic stress intensity factor for a crack propagating in a finite two-dimensional body can be computed relatively inexpensively with an accuracy sufficient for many practical purposes. Very close agreements between the K_{ID} obtained by the generation and by the propagation calculations should dispel the reservations [16,17] about this dynamic fracture algorithm.

When used in conjunction with measured crack position versus time data, the generation method with proper care can be used to accurately calculate the dynamic stress intensity factor during the fast crack propagation and crack arrest.

On the other hand the uncertainty in the K_{ID} versus $\underline{\dot{a}}$ relations, particularly in the region of very low velocities together with limitation in the finite element modeling of dynamic crack propagation offers little chance for simulating the crack propagation and crack arrest event by the propagation method when the dynamic stress intensity factor oscillates in a narrow range about the crack arrest stress intensity factor as shown by some experimental results with the single edged notch specimens reported in [25].

DISCUSSION

It has been a common practice by all, including the authors, to verify their fracture dynamic code by analyzing the Broberg problem [15] for which the dynamic solution is available. Good agreements in these studies cannot be construed as verification of numerical solutions generated for cracks propagating in finite specimens composed of real materials. The discrepancies between the computed and the experimentally determined K_{ID}-values shown in Figures 6 and 9 could have arisen from the viscous damping in Araldite B which was not modeled in the elasto-dynamic analyses described in this paper. A study of the time-dependent energy balance during crack propagation and arrest suggests that the consistently appearing second maxima in the calculated K_{ID}-curves are real phenomena based on elastic analyses. It is interesting to note that the limited experimental K_{ID} versus $\underline{a}$ relation obtained for RDCB specimens machined from high strength steel [25] is in qualitative agreement with our elastic analysis of the RDCB specimen.

ACKNOWLEDGEMENT

The results of this investigation were obtained in a reasearch contract funded by the Office of Naval Research under Contract No. N00014-76-C-0060, NR 064-478. The authors wish to acknowledge the support and encouragement of Dr. N. R. Perrone of ONR during the course of this investigation. The first author, Dr. L. Hodulak, was supported by a post-doctoral fellowship from the Deutsche Forschungsgemeinschaft, FRG. The authors also wish to acknowledge the discussions with Dr. J. F. Kalthoff, Institut für Festkörpermechanik.

REFERENCES

1. Key, S.W., "HONDO, A Finite Element Computer Program for the Large Deformation Dynamic Responses of Axisymmetric Solids," Sandia Laboratories.

2. Kobayashi, A.S., Emery, A.F. and Mall, S., "Dynamic Finite Element and Dynamic Photoelastic Analysis of Two Fracturing Homalite-100 Plates," Experimental Mechanics, Vol. 16, No. 9, pp. 321-328, September 1976.

3. Kobayashi, A.S., Emery, A.F. and Mall, S., "Dynamic Finite Element and Dynamic Photoelastic Analyses of Crack Arrest in Homalite-100 Plates," Fast Fracture and Crack Arrest, ASTM STP 627, pp. 95-108, July 1977.

4. Urabe, Y., Kobayashi, A.S., Emery, A.F. and Love, W.J., "Dynamic Finite Element Analysis of Tapered DCB Specimen," Fracture Mechanics and Technology edited by G.C. Sih and C.L. Chow, Sijthoff and Noordhoff Int. 1977, Vol. II, pp. 1499-1512.

5. Urabe, Y., Kobayashi, A.S., Emery, A.F. and Love, W.J., "Further Dynamic Finite Element Analysis of a Tapered DCB Specimen," J. of Eng. Materials and Technology, Trans of ASME, Vol. 99, Series H, No. 4, October 1977, pp. 324-328.

6. Kobayashi, A.S., Mall, S., Urabe, Y., and Emery, A.F., "A Numerical Dynamic Fracture Analysis of Three Wedge-Loaded DCB Specimens," Numerical Methods in Fracture Mechanics, edited by A.R. Luxmoore and D.R.J. Owens, University College of Swansea, January 1978, pp. 673-684.

7. Kanazawa, T., Kobayashi, A.S., Machida, S. and Urabe, Y., "Fracture Dynamic Analysis of Crack Arrest Test Specimens," ibid loc cit, pp. 709-720.

8. Keegstra, P.N.R., "A Transient Finite Element Crack Propagation Model for Nuclear Reactor Pressure Vessel Steels," J. Inst. Nucl. Engrs., Vol. 17, No. 4, pp. 89-96, 1976.

9. Keegstra, P.N.R., Head, J.L. and Turner, C.E., "A Transient Finite Element Analysis of Unstable Crack Propagation in Some 2-Dimensional Geometries," Proc. of the 4th Int'l. Conf. on Fracture, University of Waterloo Press, Vol. 3, pp. 515-522, 1977.

10. Keegstra, P.N.R., Head, J.L. and Turner, C.E., "The Interpretation of the Instrumented Charpy Test," Trans. of the 4th Int'l. Conf. on Structural Mechanics in Reactor Technology, Vol. G., CECA, CEE, CEEA Luxembourg, paper G 4/7, 1977.

11. Malluck, J.F. and King, W.W., "Fast Fracture Simulated by a Finite Element Analysis which Accounts for Crack Tip Energy Dissipation," ibid loc cit, pp. 648-659.

12. Rydholm, G., Fredriksson, B. and Nilsson, F., "Numerical Investigations of Rapid Crack Propagation," ibid loc cit, pp. 660-672.

13. Malluck, J.F. and King, W.W., "Finite Element Simulations of Fundamental Fast Fracture Problems," a paper presented at the ASTM Committee E-24 Symposium on Crack Arrest Methodology and Applications, Philadelphia, Nov. 6-7, 1978.

14. Urabe, Y., private communication.

15. Borberg, K.B., "The Propagation of a Brittle Crack," Arkiv fur Fysik, Vol. 18, pp. 159-198, 1960.

16. Kanninen, M.F., "A Critical Appraisal of Solution Techniques in Dynamic Fracture Mechanics," Numerical Methods in Fracture Mechanics, edited by A.R. Luxmoore and D.R.J. Owens, University College of Swansea, Jan. 1978, pp. 612-633.

17. Kanninen, M.F., Rosenfield, A.R., McGuire, P.M. and Barnes, R.C., "The Determination of Dynamic Fracture Toughness Values and Evaluation of Crack Arrest Concepts Using DCB Test Specimens," a paper presented at the ASTM Committee E-24 Symposium on Crack Arrest Methodology and Applications, Philadelphia, Nov. 6-7, 1978.

18. Kanninen, M.F., "A Dynamic Analysis of Unstable Crack Propagation and Arrest in the DCB Test Specimen," Int'l. J. of Fracture, Vol. 10, No. 3, pp. 415-431, September 1974.

19. Hahn, G.T., Hoagland, R.G., Kannen, M.F. and Rosenfield, A.R., "Pilot Study of Fracture Arrest Capabilities of A533B Steel," Cracks and Fracture, ASTM STP 601, pp. 209-233, June 1976.

20. Hoagland, R.G., Gehlen, P.C., Rosenfield, A.F. and Hahn, G.T., "Characteristics of a Run-Arrest Segment of Crack Extension," Fast Fracture and Crack Arrest, ASTM STP 627, pp. 203-207, July 1977.

21. Hahn, G.T., Hoagland, R.G. and Rosenfield, A.R., "A Fracture Mechanics Practice for Crack Arrest," Trans. of the 4th Int'l. Conf. on Structural Mechanics in Reactor Technology, CECA, CEE, CEEA Luxembourg, Paper G 1/6, 1977.

22. Kanninen, M.F., Popelar, C. and Gehlen, R.C., "Dynamic Analysis of Crack Propagation in the DCB Specimen," Fast Fracture and Crack Arrest, ASTM STP 627, pp. 19-38, July 1977.

23. Hahn, G.T., Gehlen, R.C., Hoagland, R.G., Marshall, C.W., Kanninen, M.F., Pipelar, C. and Rosenfield, A.F., "Critical Experiments, Measurements and Analyses to Establish a Crack Arrest Methodology for Nuclear Pressure Vessel Steels," Task 62, Second Annual Report, Battelle Columbus Laboratories BMI-1959, October 1976.

24. Kalthoff, J., Beinert, J. and Winkler, S., "Measurements of Dynamic Stress Intensity Factors for Fast Running and Arresting Cracks in Double-Cantilever-Beam Specimens," Fast Fracture and Crack Arrest, ASTM STP 627, pp. 161-176, July 1977.

25. Kalthoff, J.F., Beinert, J., and Winkler, S., "Experimental Analysis of Dynamic Effects in Different Crack Arrest Specimen," a paper presented at the ASTM E-24 Symposium on Crack Arrest Methodology and Applications, Philadelphia, Nov. 6-7, 1978.

26. Kobayashi, A.S., Urabe, Y., Emery, A.F., and Love, W.J., "Dynamic Finite Element Analyses of Two Compact Specimens," J. of Engineering Materials and Technology, Trans. of ASME, Vol. 100, No. 4, Oct. 1978, pp. 402-410.

27. Freund, L.B., "Crack Propagation in an Elastic Solid Subjected to General Loading-II Non-Uniform Rate of Extension," J. of Mechanics and Physics of Solids, Vol. 20, 1972, pp. 141-152.

28. Broberg, K.B., "The Propagating of a Brittle Crack," Arkiv fur Fysik, Vol. 18, 1960, pp. 159-198.

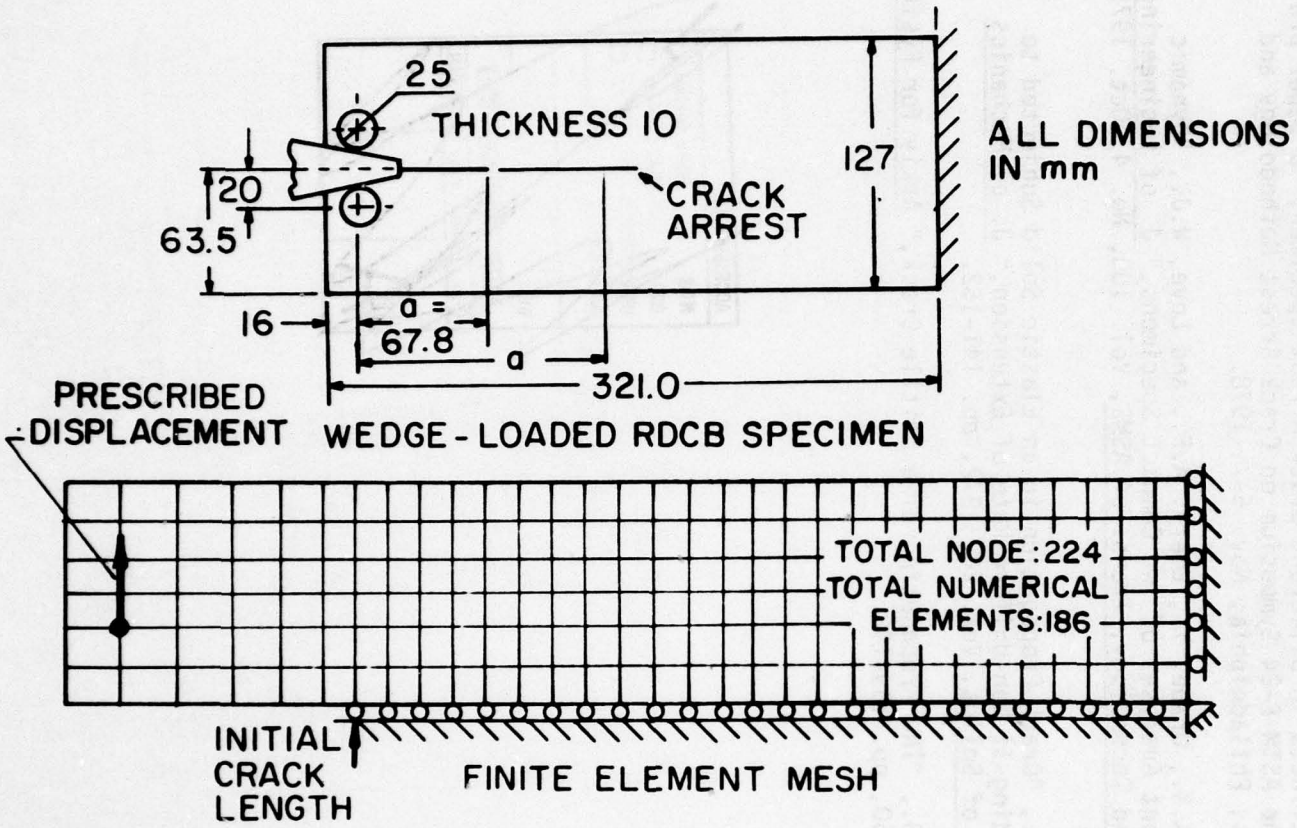

FIGURE 1. WEDGE-LOADED RDCB SPECIMEN.

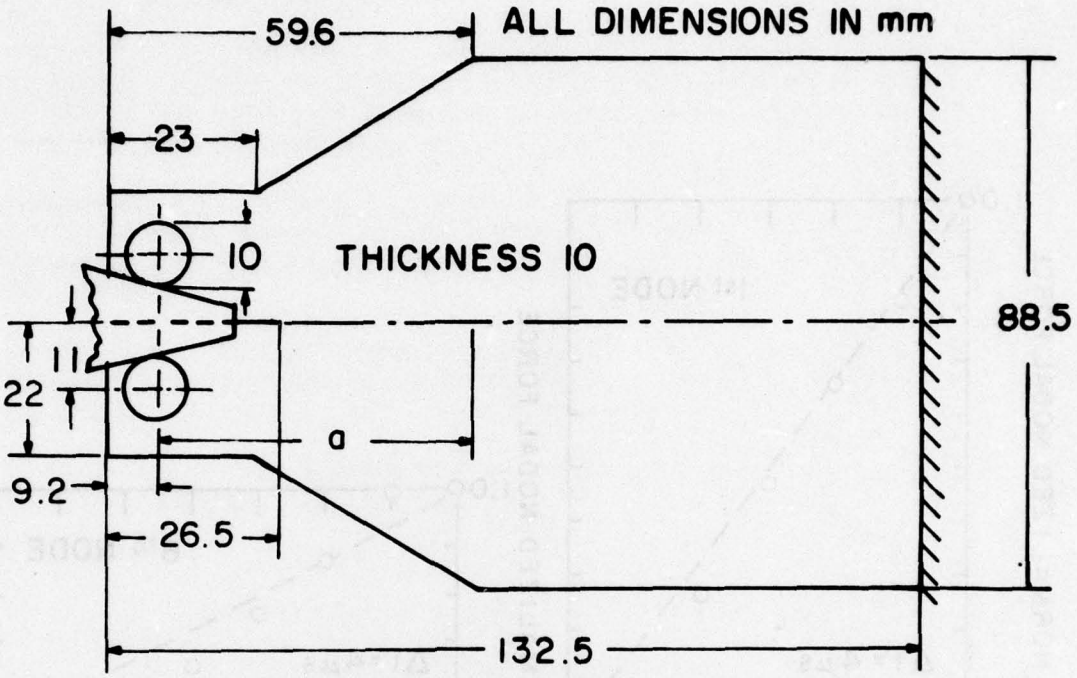

WEDGE-LOADED TDCB SPECIMEN

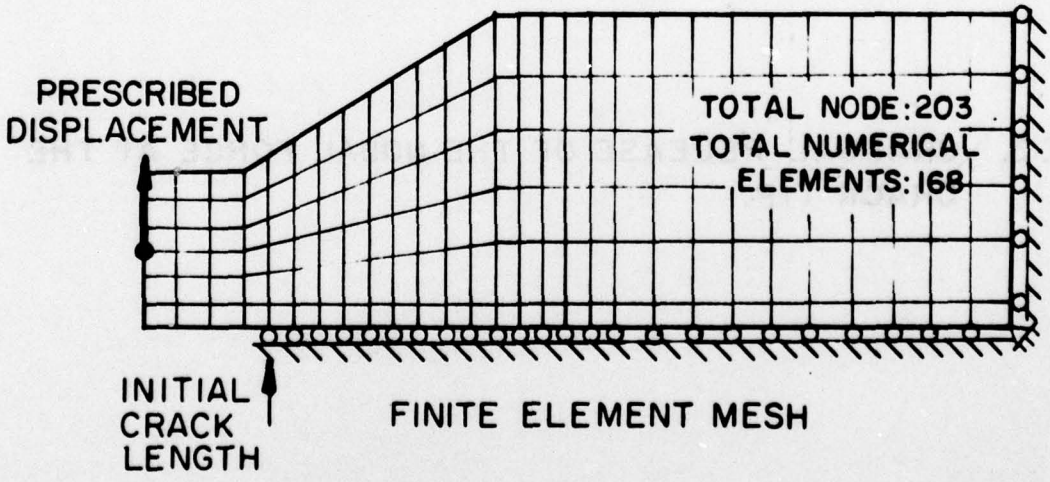

FIGURE 2. WEDGE-LOADED TDCB SPECIMEN.

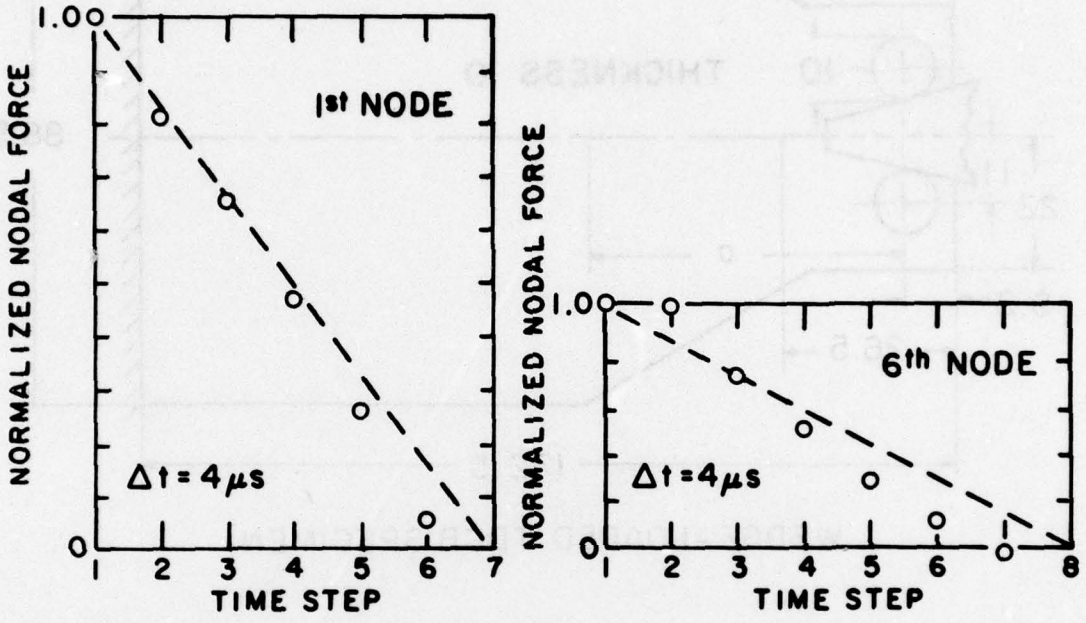

FIGURE 3. GRADUAL RELEASE OF THE NODAL FORCE AT THE CRACK TIP.

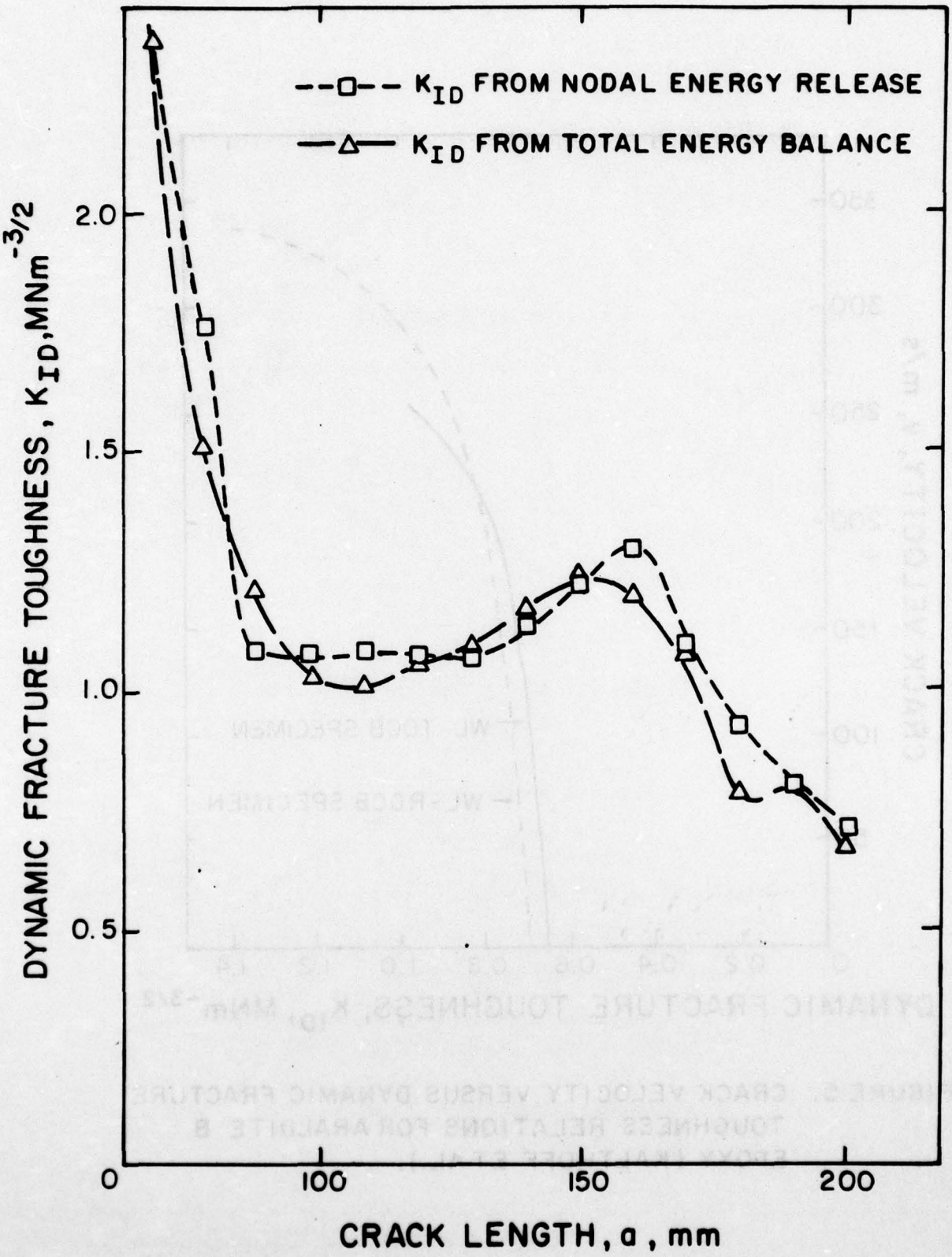

FIGURE 4. DYNAMIC FRACTURE TOUGHNESS IN WEDGE-LOADED RDCB SPECIMEN.

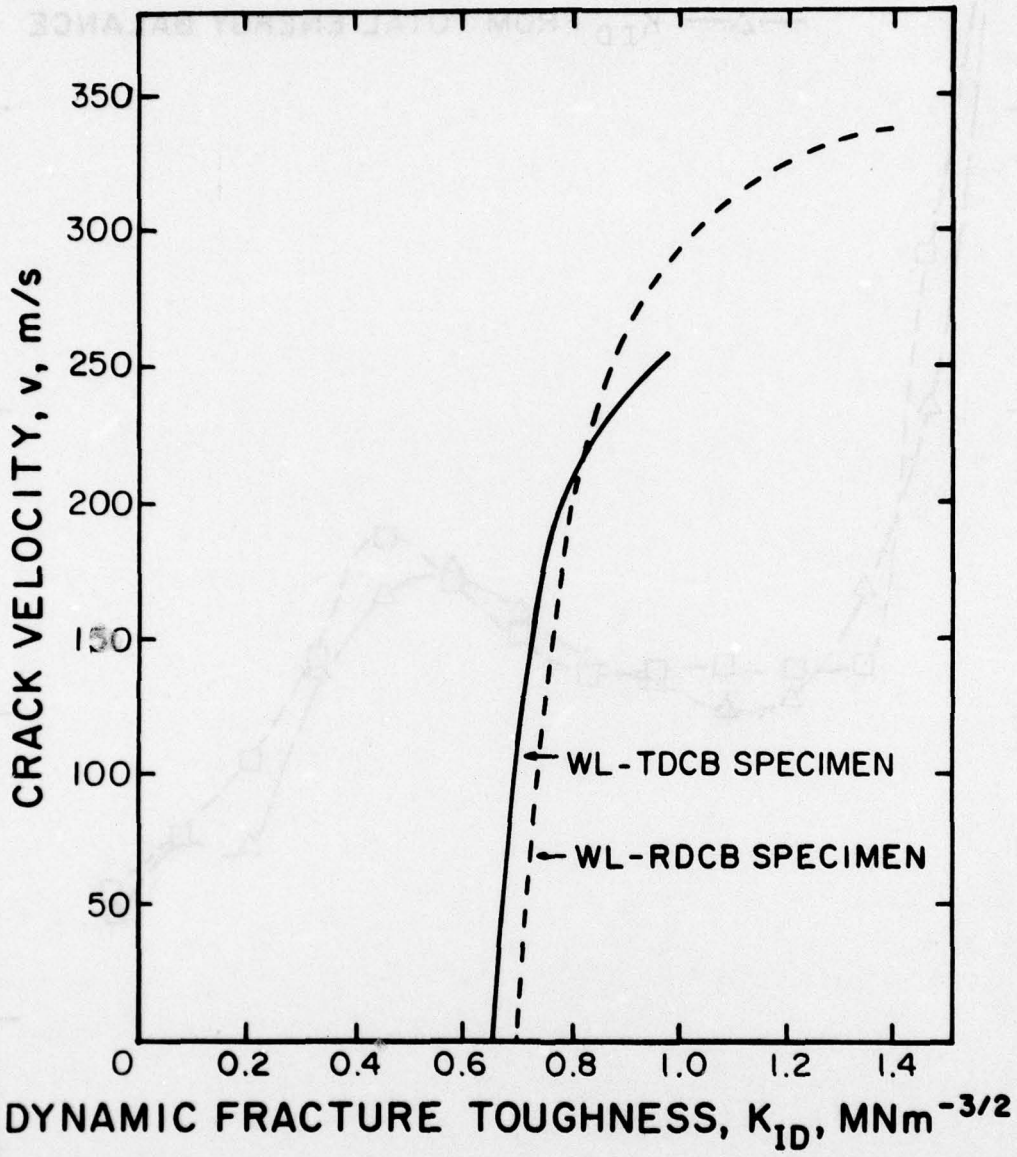

FIGURE 5. CRACK VELOCITY VERSUS DYNAMIC FRACTURE TOUGHNESS RELATIONS FOR ARALDITE B EPOXY (KALTHOFF ET AL.).

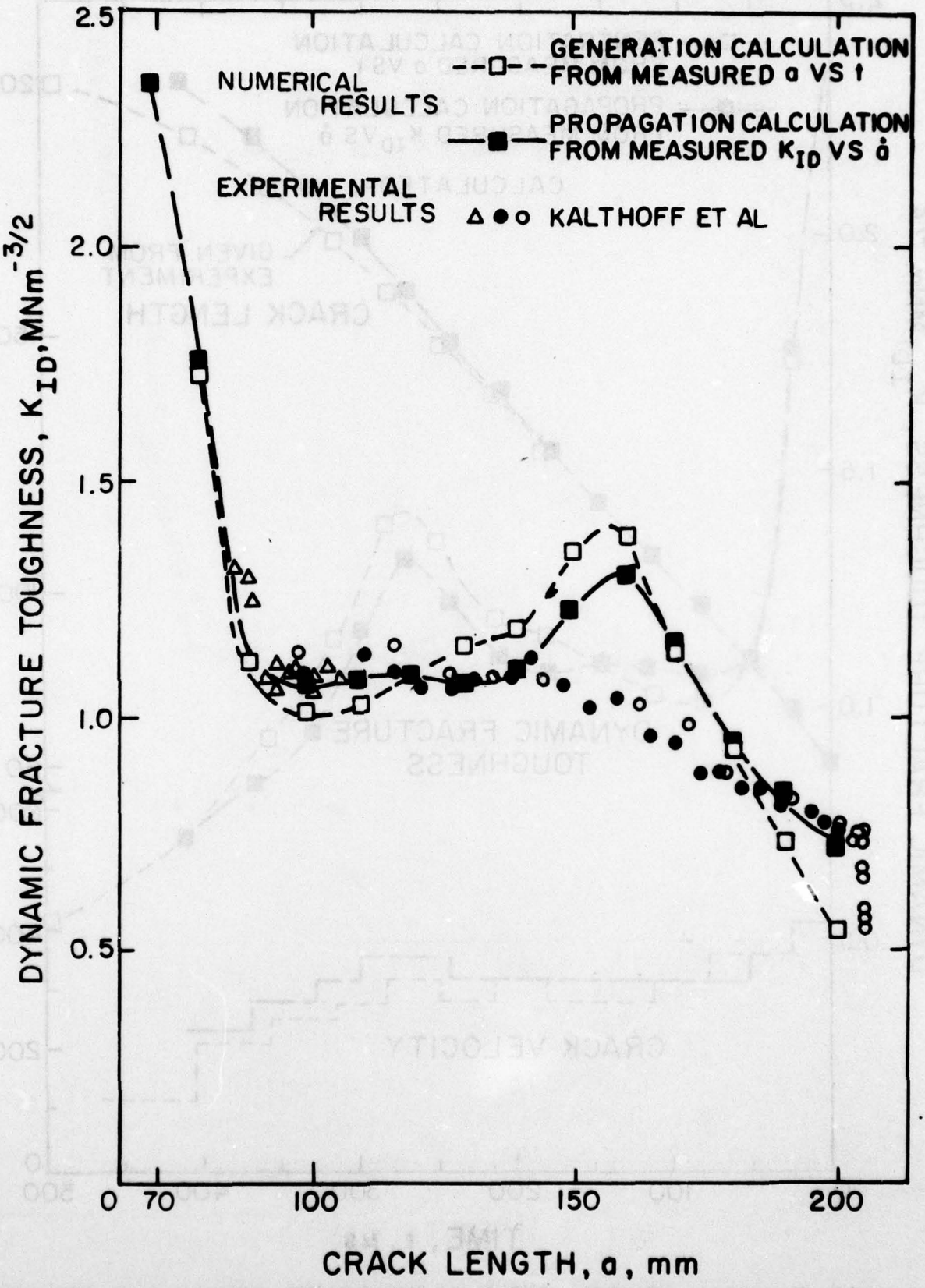

FIGURE 6. DYNAMIC FRACTURE TOUGHNESS IN WEDGE-LOADED RDCB SPECIMEN.

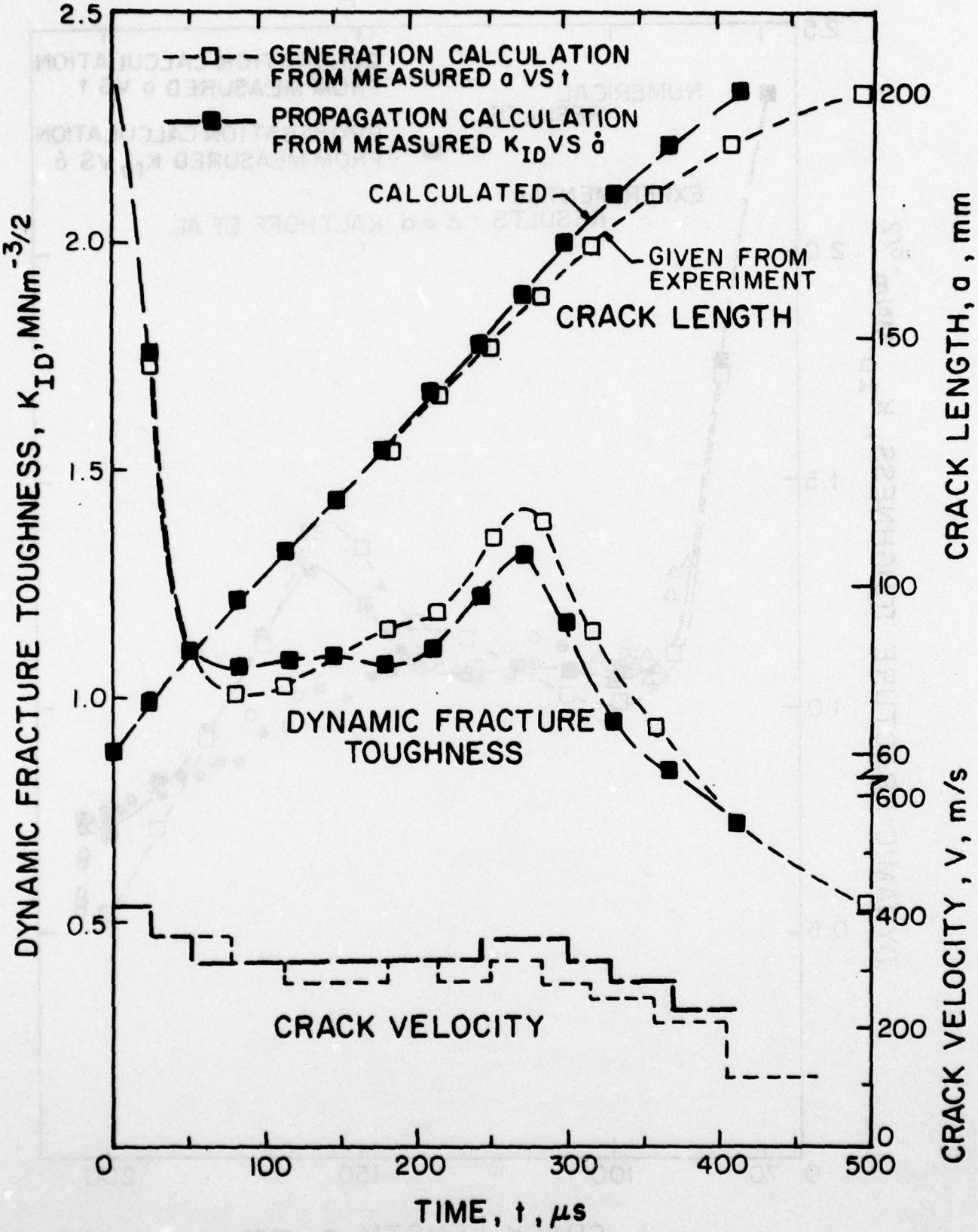

FIGURE 7. CRACK LENGTH, DYNAMIC FRACTURE TOUGHNESS AND CRACK VELOCITY VERSUS TIME IN WEDGE-LOADED RDCB SPECIMEN.

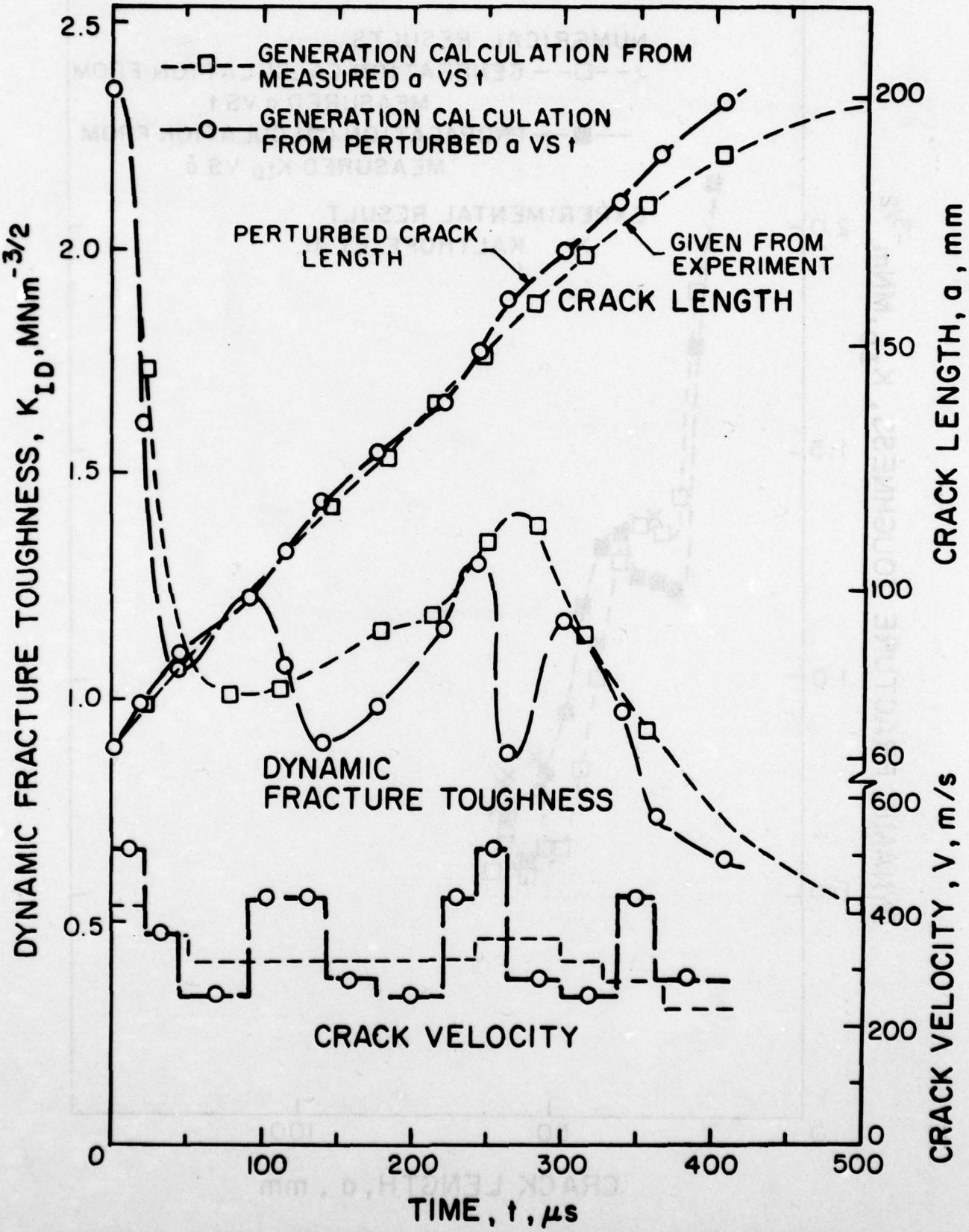

FIGURE 8. CRACK LENGTH, DYNAMIC FRACTURE AND CRACK VELOCITY VERSUS TIME IN WEDGE-LOADED RDCB SPECIMEN.

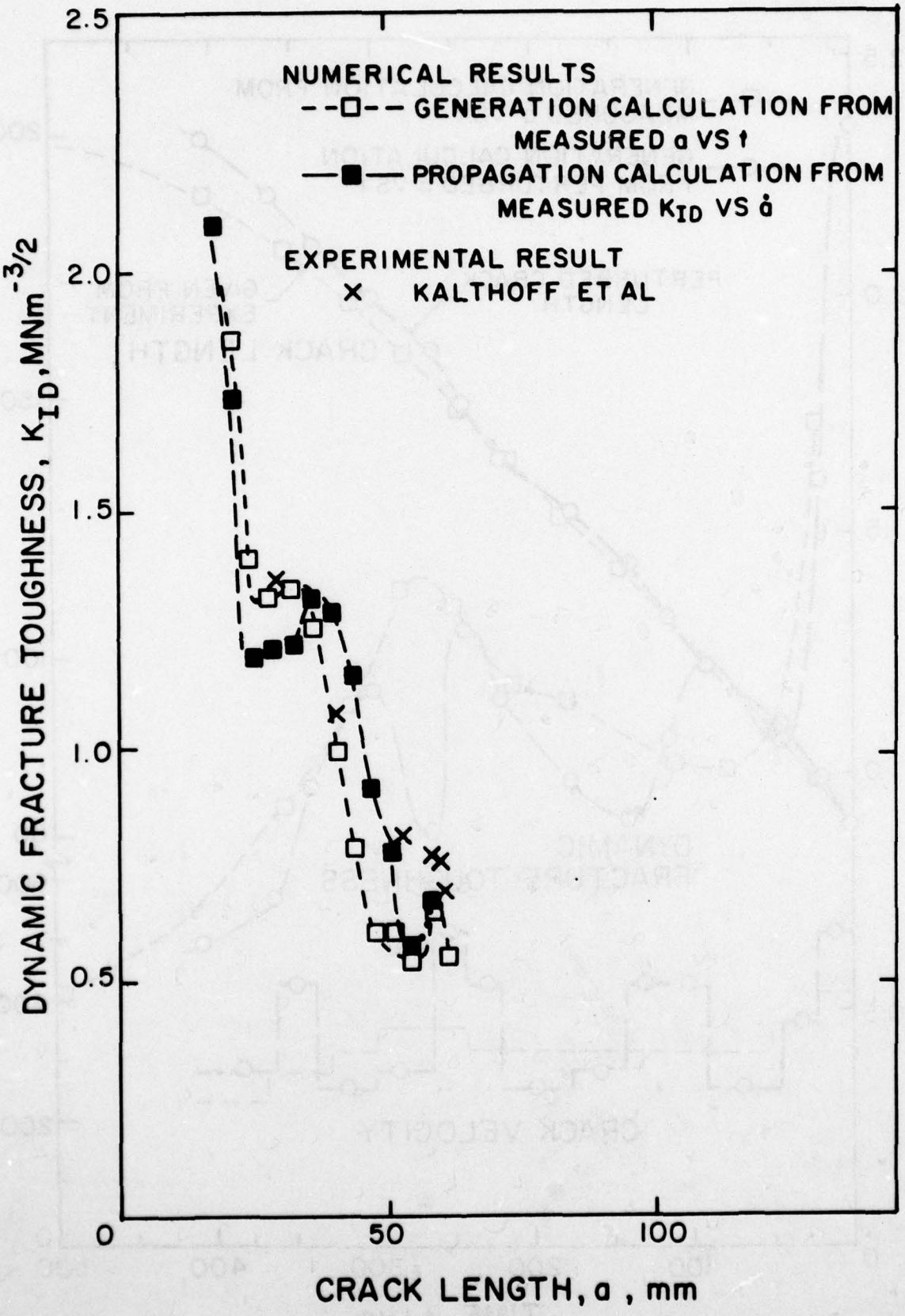

FIGURE 9. DYNAMIC FRACTURE TOUGHNESS IN WEDGE - LOADED TAPERED DCB SPECIMEN.

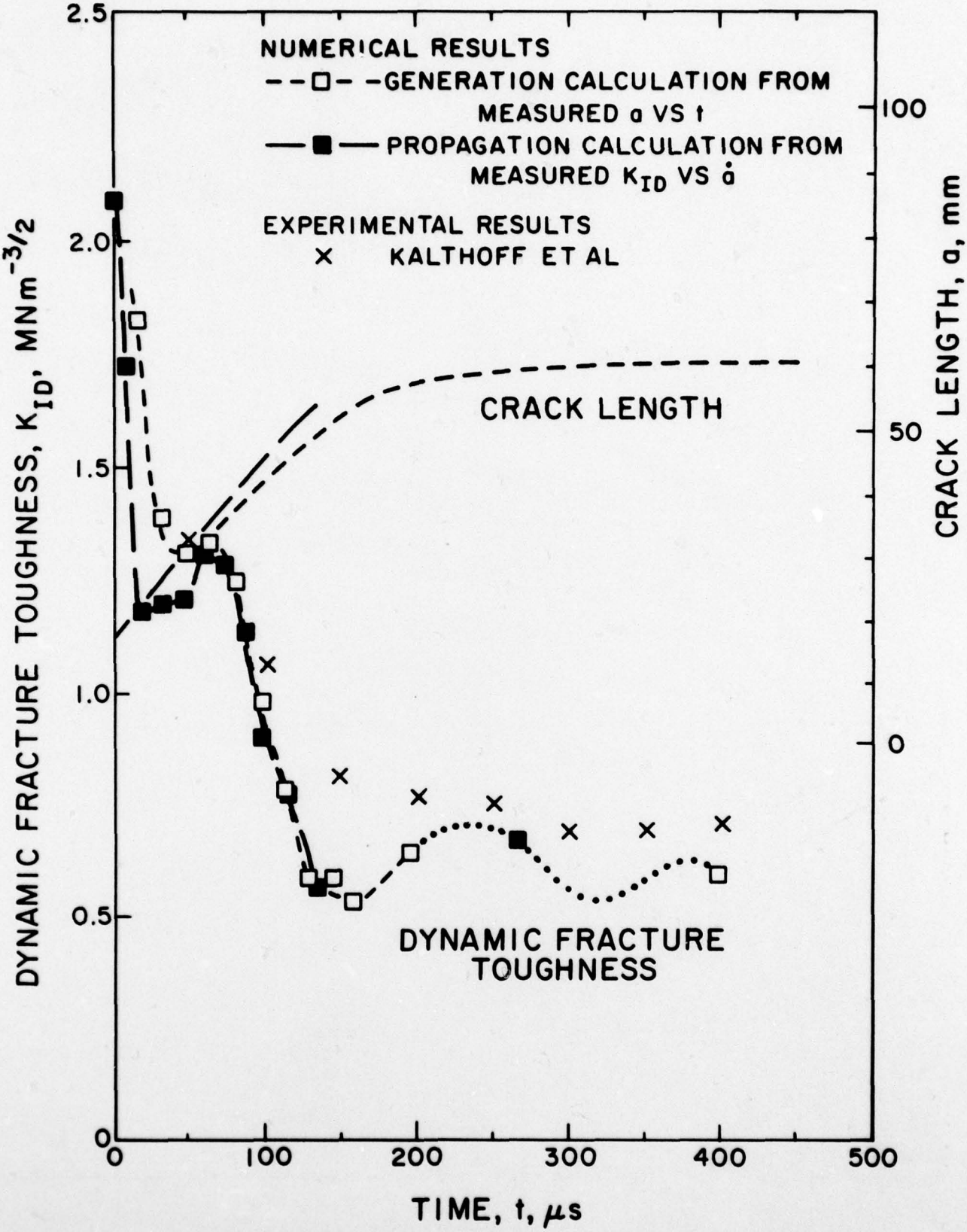

FIGURE 10. DYNAMIC FRACTURE TOUGHNESS AND CRACK LENGTH VERSUS TIME IN WEDGE-LOADED TAPERED DCB SPECIMEN.

PART 1 - Government

Administrative and Liaison Activities

Office of Naval Research
Department of the Navy
Arlington, VA 22217
Attn: Code 474 (2)
Code 471
Code 200

Director
Office of Naval Research
Branch Office
666 Summer Street
Boston, MA 02210

Director
Office of Naval Research
Branch Office
536 South Clark Street
Chicago, IL 60605

Director
Office of Naval Research
New York Area Office
715 Broadway - 5th Floor
New York, NY 10003

Director
Office of Naval Research
Branch Office
1030 East Green Street
Pasadena, CA 91106

Naval Research Laboratory (6)
Code 2627
Washington, DC 20375

Defense Documentation Center (12)
Cameron Station
Alexandria, VA 22314

Navy

Undersea Explosion Research Division
Naval Ship Research and Development Center
Norfolk Naval Shipyard
Portsmouth, VA 23709
Attn: Dr. E. Palmer, Code 177

Navy (Con't.)

Naval Research Laboratory
Washington, DC 20375
Attn: Code 8400
8410
8430
8440
6300
6390
6380

David W. Taylor Naval Ship Research and Development Center
Annapolis, MD 21402
Attn: Code 2740
28
281

U.S. Naval Weapons Center
China Lake, CA 93555
Attn: Code 4062
4520

Commanding Officer
U.S. Naval Civil Engineering Laboratory
Code L31
Port Hueneme, CA 93041

Naval Surface Weapons Center
White Oak
Silver Spring, MD 20910
Attn: Code R-10
G-402
K-82

Technical Director
Naval Ocean Systems Center
San Diego, CA 92152

Supervisor of Shipbuilding
U.S. Navy
Newport News, VA 23607

U.S. Navy Underwater Sound Reference Division
Naval Research Laboratory
P.O. Box 8337
Orlando, FL 32806

Navy (Con't.)

Chief of Naval Operations
Department of the Navy
Washington, DC 20350
Attn: Code OP-098

Strategic Systems Project Office
Department of the Navy
Washington, DC 20376
Attn: NSP-200

Naval Air Systems Command
Department of the Navy
Washington, DC 20361
Attn: Code 5302 (Aerospace and Structures)
604 (Technical Library)
3208 (Structures)

Naval Air Development Center
Director, Aerospace Mechanics
Warminster, PA 18974

U.S. Naval Academy
Engineering Department
Annapolis, MD 21402

Naval Facilities Engineering Command
200 Stovall Street
Alexandria, VA 22332
Attn: Code 03 (Research and Development)
04B
045
14114 (Technical Library)

Naval Sea Systems Command
Department of the Navy
Washington, DC 20362
Attn: Code 03 (Research and Technology)
037 (Ship Silencing Division)
035 (Mechanics and Materials)

Naval Ship Engineering Center
Department of the Navy
Washington, DC 20362
Attn: Code 6105G
6114
6120D
6128
6129

Commanding Officer and Director
David W. Taylor Naval Ship Research and Development Center
Bethesda, MD 20084
Attn: Code 042
17
172
173
174
1800
1844
1102.1
1900
1901
1945
1960
1962

Naval Underwater Systems Center
Newport, RI 02840
Attn: Dr. R. Trainor

Naval Surface Weapons Center
Dahlgren Laboratory
Dahlgren, VA 22448
Attn: Code G04
G20

Technical Director
Mare Island Naval Shipyard
Vallejo, CA 94592

U.S. Naval Postgraduate School
Library
Code 0384
Monterey, CA 93940

Webb Institute of Naval Architecture
Attn: Librarian
Crescent Beach Road, Glen Cove
Long Island, NY 11542

Army

Commanding Officer (2)
U.S. Army Research Office
P.O. Box 12211
Research Triangle Park, NC 27709
Attn: Mr. J. J. Murray, CRD-AA-IP

Watervliet Arsenal
MAGGS Research Center
Watervliet, NY 12189
Attn: Director of Research

U.S. Army Materials and Mechanics Research Center
Watertown, MA 02172
Attn: Dr. R. Shea, DRXMR-T

U.S. Army Missile Research and Development Center
Redstone Scientific Information Center
Chief, Document Section
Redstone Arsenal, AL 35809

Army Research and Development Center
Fort Belvoir, VA 22060

Air Force

Commander WADD
Wright-Patterson Air Force Base
Dayton, OH 45433
Attn: Code WWRMDD
AFFDL (FDDS)
Structures Division
AFLC (MCEEA)

Chief Applied Mechanics Group
U.S. Air Force Institute of Technology
Wright-Patterson Air Force Base
Dayton, OH 45433

Chief, Civil Engineering Branch
WLRC, Research Division
Air Force Weapons Laboratory
Kirtland Air Force Base
Albuquerque, NM 87117

Air Force Office of Scientific Research
Bolling Air Force Base
Washington, DC 20332
Attn: Mechanics Division

Department of the Air Force
Air University Library
Maxwell Air Force Base
Montgomery, AL 36112

NASA

National Aeronautics and Space Administration
Structures Research Division
Langley Research Center
Langley Station
Hampton, VA 23365

National Aeronautics and Space Administration
Associate Administrator for Advanced Research and Technology
Washington, DC 20546

Scientific and Technical Information Facility
NASA Representative (S-AK/DL)
P.O. Box 5700
Bethesda, MD 20014

Other Government Activities

Commandant
Chief, Testing and Development Division
U.S. Coast Guard
1300 E Street, NW
Washington, DC 20226

Technical Director
Marine Corps Development and Education Command
Quantico, VA 22134

Director Defense Research and Engineering
Technical Library
Room 3C128
The Pentagon
Washington, DC 20301

Director
National Bureau of Standards
Washington, DC 20034
Attn: Mr. B. L. Wilson, EM 219

Dr. M. Gaus
National Science Foundation
Environmental Research Division
Washington, DC 20550

Library of Congress
Science and Technology Division
Washington, DC 20540

Director
Defense Nuclear Agency
Washington, DC 20305
Attn: SPSS

Mr. Jerome Persh
Staff Specialist for Materials and Structures
OUSDR&E, The Pentagon
Room 3D1089
Washington, DC 20301

Chief, Airframe and Equipment Branch
FS-120
Office of Flight Standards
Federal Aviation Agency
Washington, DC 20553

National Academy of Sciences
National Research Council
Ship Hull Research Committee
2101 Constitution Avenue
Washington, DC 20418
Attn: Mr. A. R. Lytle

National Science Foundation
Engineering Mechanics Section
Division of Engineering
Washington, DC 20550

Picatinny Arsenal
Plastics Technical Evaluation Center
Attn: Technical Information Section
Dover, NJ 07801

Maritime Administration
Office of Maritime Technology
14th and Constitution Ave., NW
Washington, DC 20230

Maritime Administration
Office of Ship Construction
14th and Constitution Ave., NW
Washington, DC 20230

PART 2 - Contractors and Other Technical Collaborators

Universities

Dr. Tinsley Oden
University of Texas at Austin
345 Engineering Science Building
Austin, TX 78712

Professor Julius Miklowitz
California Institute of Technology
Division of Engineering
and Applied Sciences
Pasadena, CA 91109

Dr. Harold Liebowitz, Dean
School of Engineering and
Applied Science
George Washington University

Professor Eli Sternberg
California Institute of Technology
Division of Engineering and
Applied Sciences
Pasadena, CA 91109

Professor Paul M. Naghdi
University of California
Department of Mechanical Engineering
Berkeley, CA 94720

Professor A. J. Durelli
Oakland University
School of Engineering
Rochester, MI 48063

Professor F. L. DiMaggio
Columbia University
Department of Civil Engineering
New York, NY 10027

Professor Norman Jones
Massachusetts Institute of Technology
Department of Ocean Engineering
Cambridge, MA 02139

Professor E. J. Skudrzyk
Pennsylvania State University
Applied Research Laboratory
Department of Physics
State College, PA 16801

Professor J. Kempner
Polytechnic Institute of New York
Department of Aerospace Engineering and
Applied Mechanics
333 Jay Street
Brooklyn, NY 11201

Professor J. Klosner
Polytechnic Institute of New York
Department of Aerospace Engineering and
Applied Mechanics
333 Jay Street
Brooklyn, NY 11201

Professor R. A. Schapery
Texas A&M University
Department of Civil Engineering
College Station, TX 77843

Professor Walter D. Pilkey
University of Virginia
Research Laboratories for the
Engineering Sciences
School of Engineering and
Applied Sciences
Charlottesville, VA 22901

Professor K. D. Willmert
Clarkson College of Technology
Department of Mechanical Engineering
Potsdam, NY 13676

Dr. Walter E. Haisler
Texas A&M University
Aerospace Engineering Department
College Station, TX 77843

Dr. Hussein A. Kamel
University of Arizona
Department of Aerospace and
Mechanical Engineering
Tucson, AZ 85721

Dr. S. J. Fenves
Carnegie-Mellon University
Department of Civil Engineering
Schenley Park
Pittsburgh, PA 15213

Universities (Con't.)

Professor H. W. Liu
Syracuse University
Department of Chemical Engineering
and Metallurgy
Syracuse, NY 13210

Professor S. Bodner
Technion R&D Foundation
Haifa, Israel

Professor Werner Goldsmith
University of California
Department of Mechanical Engineering
Berkeley, CA 94720

Professor R. S. Rivlin
Lehigh University
Center for the Application
of Mathematics
Bethlehem, PA 18015

Professor F. A. Cozzarelli
State University of New York at Buffalo
Division of Interdisciplinary Studies
Karr Parker Engineering Building
Chemistry Road
Buffalo, NY 14214

Professor Joseph L. Rose
Drexel University
Department of Mechanical Engineering
and Mechanics
Philadelphia, PA 19104

Professor B. K. Donaldson
University of Maryland
Aerospace Engineering Department
College Park, MD 20742

Professor Joseph A. Clark
Catholic University of America
Department of Mechanical Engineering
Washington, DC 20064

Professor T. C. Huang
University of Wisconsin-Madison
Department of Engineering Mechanics
Madison, WI 53706

Dr. Samuel B. Batdorf
University of California
School of Engineering
and Applied Science
Los Angeles, CA 90024

Professor Isaac Fried
Boston University
Department of Mathematics
Boston, MA 02215

Professor Michael Pappas
New Jersey Institute of Technology
Newark College of Engineering
323 High Street
Newark, NJ 07102

Professor E. Krempl
Rensselaer Polytechnic Institute
Division of Engineering
Engineering Mechanics
Troy, NY 12181

Dr. Jack R. Vinson
University of Delaware
Department of Mechanical and Aerospace
Engineering and the Center for
Composite Materials
Newark, DL 19711

Dr. Dennis A. Nagy
Princeton University
School of Engineering and Applied Science
Department of Civil Engineering
Princeton, NJ 08540

Dr. J. Duffy
Brown University
Division of Engineering
Providence, RI 02912

Dr. J. L. Swedlow
Carnegie-Mellon University
Department of Mechanical Engineering
Pittsburgh, PA 15213

Dr. V. K. Varadan
Ohio State University Research Foundation
Department of Engineering Mechanics
Columbus, OH 43210

Universities (Con't.)

Dr. Ronald L. Huston
Department of Engineering Analysis
University of Cincinnati
Cincinnati, OH 45221

Professor G. C. M. Sih
Lehigh University
Institute of Fracture and
Solid Mechanics
Bethlehem, PA 18015

Professor Albert S. Kobayashi
University of Washington
Department of Mechanical Engineering
Seattle, WA 98105

Professor Daniel Frederick
Virginia Polytechnic Institute and
State University
Department of Engineering Mechanics
Blacksburg, VA 24061

Professor A. C. Eringen
Princeton University
Department of Aerospace and
Mechanical Sciences
Princeton, NJ 08540

Professor E. H. Lee
Stanford University
Division of Engineering Mechanics
Stanford, CA 94305

Professor Albert I. King
Wayne State University
Biomechanics Research Center
Detroit, MI 48202

Dr. V. R. Hodgson
Wayne State University
School of Medicine
Detroit, MI 48202

Dean B. A. Boley
Northwestern University
Department of Civil Engineering
Evanston, IL 60201

Professor P. C. Hodge, Jr.
University of Minnesota
Department of Aerospace Engineering
and Mechanics
Minneapolis, MN 55455

Dr. D. Drucker
University of Illinois
Dean of Engineering
Urbana, IL 61801

Professor S. M. Spearing
University of Illinois
Department of Civil Engineering
Urbana, IL 61801

Professor [illegible]
University of California, San Diego
Department of Applied Mechanics
La Jolla, CA 92037

Professor William A. Nash
University of Massachusetts
Department of Mechanics and
Aerospace Engineering
Amherst, MA 01003

Professor G. [illegible]
Stanford University
Department of Applied Mechanics
Stanford, CA 94305

Professor T. J. Akhtarzad
Northwestern University
Department of Civil Engineering
Evanston, IL 60201

Professor S. F. Ravi
University of California
Department of Mechanics
Los Angeles, CA 90024

Professor Burt Paul
University of Pennsylvania
Towne School of Civil and
Mechanical Engineering
Philadelphia, PA 19104

Universities (Con't.)

Dr. Z. Hashin
University of Pennsylvania
Department of Metallurgy and
Materials Science
College of Engineering and
Applied Science
Philadelphia, PA 19104

Dr. Jackson C. S. Yang
University of Maryland
Department of Mechanical Engineering
College Park, MD 20742

Professor T. Y. Chang
University of Akron
Department of Civil Engineering
Akron, OH 44325

Professor Charles W. Bert
University of Oklahoma
School of Aerospace, Mechanical,
and Nuclear Engineering
Norman, OK 73019

Professor Satya N. Atluri
Georgia Institute of Technology
School of Engineering Science and
Mechanics
Atlanta, GA 30332

Professor Graham F. Carey
University of Texas at Austin
Department of Aerospace Engineering
and Engineering Mechanics
Austin, TX 78712

Industry and Research Institutes

Dr. Jackson C. S. Yang
Advanced Technology and Research, Inc.
10006 Green Forest Drive
Adelphi, MD 20783

Dr. Norman Hobbs
Kaman AviDyne
Division of Kaman
Sciences Corp.
Burlington, MA 01803

Industry and Research Institutes (Con't.)

Argonne National Laboratory
Library Services Department
9700 South Cass Avenue
Argonne, IL 60440

Dr. M. C. Junger
Cambridge Acoustical Associates
1033 Massachusetts Avenue
Cambridge, MA 02138

Dr. V. Godino
General Dynamics Corporation
Electric Boat Division
Groton, CT 06340

Dr. J. L. Greenspon
J. G. Engineering Research Associates
3831 Menlo Drive
Baltimore, MD 21215

Dr. K. C. Park
Lockheed Missile and Space Company
3251 Hanover Street
Palo Alto, CA 94304

Newport News Shipbuilding and
Dry Dock Company
Library
Newport News, VA 23607

Dr. W. F. Bozich
McDonnell Douglas Corporation
5301 Bolsa Avenue
Huntington Beach, CA 92647

Dr. H. N. Abramson
Southwest Research Institute
8500 Culebra Road
San Antonio, TX 78284

Dr. R. C. DeHart
Southwest Research Institute
8500 Culebra Road
San Antonio, TX 78284

Dr. M. L. Baron
Weidlinger Associates
110 East 59th Street
New York, NY 10022

Industry and Research Institutes (Con't.)

Dr. T. L. Geers
Lockheed Missiles and Space Company
3251 Hanover Street
Palo Alto, CA 94304

Mr. William Caywood
Applied Physics Laboratory
Johns Hopkins Road
Laurel, MD 20810

Dr. Robert E. Nickell
Pacifica Technology
P.O. Box 148
Del Mar, CA 92014

Dr. M. F. Kanninen
Battelle Columbus Laboratories
505 King Avenue
Columbus, OH 43201

Dr. G. T. Hahn
Battelle Columbus Laboratories
505 King Avenue
Columbus, OH 43201

Dr. A. A. Hochrein
Daedalean Associates, Inc.
Springlake Research Center
15110 Frederick Road
Woodbine, MD 21797

Mr. Richard Y. Dow
National Academy of Sciences
2101 Constitution Avenue
Washington, DC 20418

Mr. H. L. Kington
Airesearch Manufacturing Company
of Arizona
P.O. Box 5217
111 South 34th Street
Phoenix, AZ 85010

Dr. M. H. Rice
Systems, Science, and Software
P.O. Box 1620
La Jolla, CA 92037

UNCLASSIFIED

SECURITY CLASSIFICATION OF THIS PAGE (When Data Entered)

REPORT DOCUMENTATION PAGE		READ INSTRUCTIONS BEFORE COMPLETING FORM
1. REPORT NUMBER TR No. 34	2. GOVT ACCESSION NO.	3. RECIPIENT'S CATALOG NUMBER TR-34
4. TITLE (and Subtitle) A Critical Examination of a Numerical Fracture Dynamic Code		5. TYPE OF REPORT & PERIOD COVERED Interim Report 6. PERFORMING ORG. REPORT NUMBER 34
7. AUTHOR(s) L. Hodulak, A.S. Kobayashi, and W.J. Love		8. CONTRACT OR GRANT NUMBER(s) N00014-76-C-0060 NR 064-478
9. PERFORMING ORGANIZATION NAME AND ADDRESS University of Washington Department of Mechanical Engineering Seattle, Washington 98195		10. PROGRAM ELEMENT, PROJECT, TASK AREA & WORK UNIT NUMBERS
11. CONTROLLING OFFICE NAME AND ADDRESS Office of Naval Research Arlington, Virginia		12. REPORT DATE February 1979 13. NUMBER OF PAGES 24
14. MONITORING AGENCY NAME & ADDRESS(if different from Controlling Office)		15. SECURITY CLASS. (of this report) Unclassified 15a. DECLASSIFICATION/DOWNGRADING SCHEDULE
16. DISTRIBUTION STATEMENT (of this Report) unlimited		
17. DISTRIBUTION STATEMENT (of the abstract entered in Block 20, if different from Report)		
18. SUPPLEMENTARY NOTES		
19. KEY WORDS (Continue on reverse side if necessary and identify by block number) Dynamic Fracture Dynamic Finite Element Analysis Dynamic Fracture Toughness Crack Arrest Stress Intensity Factor		

20. ABSTRACT (Continue on reverse side if necessary and identify by block number)

After upgrading the energy dissipation algorithm, numerical experiments were conducted to assess the reliability of the explicit dynamic finite element code, HCRACK. Two dynamic fracture specimens, i.e., the wedge-loaded rectangular DCB (RDCB) specimen and the wedge-loaded tapered DCB (TDCB) specimen, ~~which were studied experimentally by Kalthoff et al.~~, were then analyzed with this updated fracture dynamic code. Using the experimentally determined dynamic fracture toughness, K_{ID} versus crack velocity, $\dot{a}$, relation, the RDCB specimen was

(continued on separate page)

DD FORM 1 JAN 73 1473 EDITION OF 1 NOV 65 IS OBSOLETE
S/N 0102-014-6601

UNCLASSIFIED

SECURITY CLASSIFICATION OF THIS PAGE (When Data Entered)

DD form 1473

20. ABSTRACT (continued)

analyzed first by the "propagation method" where good agreements between calculated and measured K_{ID} versus a relation were observed. The calculated a versus time, t, relation was then used as input data in the "generation method" where the resultant K_{ID} were virtually identical to those obtained in the propagation method. Error analyses of the generation method were also made first by using the experimentally determined a versus t relation and secondly by artifically perturbing this relation.

A TDCB specimen was then analyzed with both the propagation and generation methods by using the K_{ID} versus $\dot{a}$ relation established for this specimen and the measured a versus t relation, respectively. The computed K_{ID} obtained by both methods were in good agreement with the experimental results, showing that either approach can be used in analyzing fracture.